Desalination and Water Treatment
www.deswater.com
doi: 10.5004/dwt.2021.26573

210 (2021) 281–295
January

Application of modified graphene oxide with thermosensitive polymers for adsorption of antibiotics from synthetic contaminated water

Payam Bahar[a], Amir Hessam Hassani[a,*], Homayon Ahmad Panahi[b], Elham Moniri[c]

[a]*Department of Environmental Engineering, Faculty of Natural Resources and Environment, Science and Research Branch, Islamic Azad University, Tehran, Iran, emails: Ahhassani.Env@yahoo.com (A.H. Hassani), payam.bahaar@yahoo.com (P. Bahar)*
[b]*Department of Chemistry, Central Tehran Branch, Islamic Azad University, Tehran, Iran, email: h.ahmadpanahi@iauctb.ac.ir (H.A. Panahi)*
[c]*Department of Chemistry, Varamin-Pishva Branch, Islamic Azad University, Varamin, Iran, email: moniri30003000@yahoo.com (E. Moniri)*

Received 23 March 2020; Accepted 6 September 2020

ABSTRACT

Present study evaluates the removal of antibiotics from contaminated water using a novel thermosensitive graphene oxide. The modified graphene oxide with Poly N-vinyl caprolactam has been characterized by different methods such as X-ray diffraction analysis, scanning electron microscopy, Fourier transform infrared spectroscopy, and Brunauer–Emmett–Teller (BET) surface area. The thermogravimetric analysis showed the melting and degradation of polymeric chains of poly N-vinyl caprolactam, which confirms the presence of surface-bonded polymer. In order to study the relationship between adsorption properties of amoxicillin (AMX) and ciprofloxacin (CIP) and effective parameters, several independent factors (pH, concentrations, temperature, and time) have been optimized. The results show that complete removal of 20 mg/L of AMX and CIP in a solution volume of 100 mL is reached within 30 min using 50 mg of the adsorbent at acidic pH values. The behavior of AMX and CIP adsorption onto the graphene oxide well fitted the pseudo-second-order kinetic model and Langmuir isotherm. The negative value of $\Delta H°$ and $\Delta G°$ (−61.76, −97.44 kJ/mol) showed that the adsorption was exothermic and spontaneous. Therefore, it can be concluded that thermosensitive graphene oxide could be a reliable adsorbent for the removal of antibiotics from contaminated water.

Keywords: Adsorption; Antibiotics; Graphen oxide; Kinetics; Poly N-vinyl caprolactam

1. Introduction

Emerging contaminants such as pharmaceuticals have been reported to be in the aquatic environment (e.g., water, sediment, and biota) whose presence or health effects have recently been considered. There is no information available on many emerging ecological information, risk assessment, and quantities in drinking water resources to predict their health effects on humans and animals [1,2]. Pharmaceuticals, pesticides, endocrine disrupting compounds, surfactants, and personal care products are among the known emerging contaminants that have been detected in surface and groundwater [3,4]. Antibiotics are recently studied by various researchers as emerging contaminants in wastewater and water resources [5]. Antibiotics production and their release from body after consumption lead to the intrusion of these compounds into the aquatic ecosystems. The residues of antibiotics in the environment have led to the growing international concern [6]. High detection frequency in the environment and bacterial resistance formation are the two main features associated with antibiotics. Therefore, in order to mitigate the potential health effect of antibiotics in the environment, their removal from wastewater is of great importance.

* Corresponding author.

Biological and physical methods have been reported to be effective techniques for the degradation and removal of organic contaminants from wastewater. However, applications of these treatment methods are limited in case of the residual pharmaceutical compound which is due to the aromaticity and the structural complexity of these compounds [7]. Consequently, other methods have been proposed for the oxidation of pharmaceuticals such as ozonation [8], advanced oxidation process [6], and ion exchange [9]. However, the application of chemical processes for the removal of the pharmaceutical may lead to the generation of intermediates suspected to be more toxic than the initial compound [10]. Adsorption of the contaminants is considered among the effective methods for the removal of antibiotics from contaminated water which is due to the simplicity of process operation, process design, high removal efficiency, complete removal without by-product generation, and lower operation costs [11]. One of the recently introduced adsorbent in organic contaminants removal is graphene oxide (GO). Presence of oxygen-containing functional groups along with high surface area of the GO makes it a reliable nanomaterial for the adsorption processes [12]. There have been different studies using the graphene oxide for adsorption of antibiotics from contaminated water [13,14]. Miao et al. [14] investigated the adsorption of tetracyclines on magnetic graphene oxide. They found that chlortetracycline was well-adsorbed at alkaline condition while, hydrochloride (TC) and oxytetracycline were effectively adsorbed in the acidic condition. Rostamian and Behnejad [15] investigated the performance of graphene oxide nanosheet for the adsorption of tetracycline, doxycycline, and ciprofloxacin (CIP). They reported that the graphene oxide nanosheet is able to adsorb the drugs in pH values of 6–7 and contact time of 100–200 min. They also reported that increasing the solution temperature from 25°C to 45°C reduced the removal efficiency.

The performance of the GO in contaminants adsorption from water could be enhanced by intrusion of the polymers into the graphene structure. Thermosensitive polymers (TSPs) are among the widely used polymers in various applications. Poly(N-vinyl caprolactam) (PNVCL) is a TSP showing a lower critical solution temperature (CST) in aqueous solutions [16].

To our knowledge, there is no study investigating the performance of thermosensitive graphene oxide (TS-GO) for adsorption of antibiotics from contaminated water. Therefore, present study aims to investigate the adsorption of amoxicillin (AMX) and CIP, as the widely used antibiotics. Accordingly, in the first step TS-GO was synthesized and characterized. Then the adsorption of the AMX and CIP was in different conditions such as solution pH, different TS-GO, and antibiotics concentrations, contact time, and temperature. Kinetics, isotherms and thermodynamics of adsorption were also investigated.

2. Materials and methods

2.1. Materials and reagents

The chemicals used for catalyst preparation and adsorption experiments in the present study were of analytical grade including P_2O_5 (Sigma-Aldrich, Germany), $K_2S_2O_8$ (Merck, Germany), graphite powder (Sigma-Aldrich, Germany), thionyl chloride (Merck, Germany), acrylamide (Sigma-Aldrich, Germany), tetrahydrofuran (Sigma-Aldrich, Germany), poly(N-vinyl caprolactam) (Sigma-Aldrich, Germany), sulfuric acid (Merck, Germany), sodium hydroxide (Merck, Germany), acrylic acid (Sigma-Aldrich, Germany), and AIBN (Sigma-Aldrich, Germany). All the experiments were conducted in duplicate and the average values have been reported.

2.2. Synthesis of adsorbent

The GO used in the present study was prepared by a modification of Hummers and Offeman's method [17,18]. Briefly saying, 2.5 g of P_2O_5 and 2.5 g of $K_2S_2O_8$ were added into an Erlenmeyer with 12.5 mL of concentrated acid sulfuric, and solution was mixed with magnetic stirrer to reach the complete dissolving of the reactants. Then, 2.5 g of graphite powder was added to the solution. Afterward, the mixture was refluxed in 80°C for about 8 h in an oil bath. Thereafter, the solution was left at room temperature to cool down. Then, 500 mL distilled water was added to the solution and the mixture was stirred for 12 h. The mixture was then washed with deionized water to remove acid and the collected solids at the bottom were dried at room temperature as synthesized GO.

For the synthesis of TS-GO, 1 g of the GO was added to 30 mL of thionyl chloride in an Erlenmeyer and sonicated for 10 min. Then, the solution was refluxed in the presence of 60 mL of acrylamide in 80°C for 72 h. After that, the solution was centrifuged and was washed with tetrahydrofuran for two times to remove the redundant thionyl chloride from the surface of GO. Then, the solution was dried in 50°C for 3 h. Afterward, the graphene oxide-acrylamide powder was refluxed in 60°C for 7 h in the presence of 40 mL of ethanol, 3 mL of acrylic acid, 10 mL of PVCL solution (PVCL solution was prepared by adding 250 mg of PVCL in 10 mL of ethanol), and 100 mg AIBN (initiator). Finally, the solution was washed with 40 mL of ethanol and then dried at room temperature. Therefore, for synthesis of TS-GO, 1 g of the GO along with 250 mg of PVCL have been used.

2.3. Adsorbent characterization

The as-prepared TS-GO adsorbent was characterized by X-ray diffraction (XRD) analysis on a STOE power diffraction system at 40 kV and 40 mA equipped with a Cu/Kα (λ = 1.54060 Å) radiation source (in a 2θ range of 10°–80°), scanning electron microscopy (SEM, XL30 Philips), Brunauer–Emmett–Teller (BET) surface area (Micromeretic/Gemini-2372 surface area analyzer), and FTIR (Shimadzu-8400S spectrometer in the range of 400–4,000 cm^{-1} using KBr pellets). Moreover, the pore size distribution was obtained from the desorption branch of the isotherm curve using the Barrett–Joyner–Halenda (BJH) model. Elemental mapping was acquired on an energy-dispersive X-ray (EDX) spectrometer connected with FE-SEM. The zeta potentials were obtained by Malvern Zetasizer Nano ZS particle analyzer. The thermogravimetric measurements (TGA) were carried out using (TGA SDTQ600) and were performed at a temperature range from 0°C to 1,000°C in air with ramp 10°C/min.

2.4. Adsorption experiments

AMX and CIP powders were used in the present study as the model contaminants of antibiotics. For conducting the experiments, 1 g/L stock solutions of the AMX and CIP antibiotics were prepared daily. The adsorption experiments were conducted in batch mode in a glass flask. In all the experiments, 50 mL of the contaminated water with known concentrations of AMX and CIP were used, and then 50 mL of the TS-GO with known concentration was added into the experiment flask and the contact time was recorded directly after TS-GO addition. At the end of the contact time, the solution was filtered using 0.45 μm paper filter. The effects of different operational parameters such as pH (3–9), TS-GO concentration (20–200 mg/L), contact time (0–150 min), antibiotics concentration (10–100 mg/L), and solution temperature (20°C–40°C) were investigated. Reusability of the catalyst was also investigated to see the ability of adsorbent for further use. Table 1 summarizes the experimental runs in the present study.

The performance of the process was investigated by antibiotics removal efficiency and the amount of adsorbed antibiotics based on Eqs. (1) and (2). Eq. (2) indicates the amount of antibiotic adsorbed on the adsorbent. While, antibiotic removal efficiency is showing the percentile of antibiotic removed from the solution.

$$\text{Antibiotic removal efficiency } (\%) = \frac{C_0 - C_t}{C_0} \times 100 \quad (1)$$

$$\text{Adsorbed antibiotics } (\text{mg/g}) = \frac{C_0 - C_t}{C_{\text{TS-GO}}} \times 1{,}000 \quad (2)$$

where C_0 and C_t are the initial and final AMX or CIP concentrations, respectively. $C_{\text{TS-GO}}$ is the concentration of the catalyst in the experiments.

2.5. Analytical methods

AMX and CIP as our target contaminants were measured using Agilent HPLC (Eclipse Plus C18 column; 3.5 μm, 4.6 mm × 100 mm). For the measurement of AMX, the mobile phase used was a volumetric ratio of 60/40 of phosphate buffer with pH = 4.6 and acetonitrile and the flow rate was adjusted to 1 mL/min. The detector used to measure AMX was UV type, which detects separated AMX at 190 nm. The mobile phase in case of CIP was a volumetric ratio of 80/20 of water/acetonitrile at a flow rate of 1 mL/min. The extracted CIP was read at 278 nm.

3. Results and discussion

3.1. Nano-sorbent preparation and characterization

In this work, a novel thermosensitive GO based adsorbent named TS-GO was synthesized in the presence of PNVCL to improve the adsorption performance. The adsorbent was prepared by sonication and reflux processes. In addition, the structural and surficial properties have been investigated to study the modified adsorption performance of TS-GO nanosheets.

The XRD pattern of the prepared GO was recorded and presented in Fig. 1. For pure GO, major peaks at 2θ values of 10.50°, 28.53°, 38.61°, and 61.43° were observed, which match well with the (111), (002), (422), and (110) crystal planes of graphene oxide, respectively [19].

The XRD patterns of the modified GO showed a well-crystallized material owing to the high intensity, narrow width, and sharpness of diffraction peaks. Fig. 2 shows the diffraction peaks at 2θ values of 19.6716°, 21.5137°, 29.8403°, and 31.3950° which are corresponded to the new planes which are originated from PNVCL and the effect of polymer on crystal structure [20]. This can verify TS-GO was prepared and PNVCL is not faded in the modification process. In addition, the peaks at 23.21° and 42.58° can be assigned to the (002) and (100) plane of graphite (JCPDS 96-901-2232). These results were in good agreement with those reported in the literature [21].

To confirm the successful synthesis and analyze the chemical structures of TS-GO nanosheets via the chemical reaction between amino groups from PNVCL and carbonyl groups from GO nanosheets, FT-IR spectra of reactants and products were recorded. As shown in Fig. 3, the band corresponding to C=O groups of carboxyl (–COOH) has appeared at 1,720 cm^{-1}. The stretching band at 3,417 cm^{-1} can be originated from the O–H stretching vibration and maybe due to the presence of the hydroxylic groups of chemisorbed water on the surface of GO. Five characteristic peaks at 601; 1,064; 1,380; 2,861; and 2,923 cm^{-1} in the spectrum of GO are attributed to the stretching and bending vibrations of aromatic C–H, C–O–C alkoxy, C–O epoxy, and aliphatic C–H bonds in the structure, respectively. The sharp characteristic peak at 1,635 cm^{-1} is ascribed to the skeletal vibration of C=C bonds [22].

Several characteristic peaks can be observed in the FTIR spectrum of TS-GO, Fig. 4. The observed peaks at 1,457 and 3,293 cm^{-1} are assigned to C–N bands and N–H bands of PNVCL polymer, respectively. Although, the characteristic stretch of C–N bond occurs at 1,457 cm^{-1}, four other peaks appears at 1,033; 1,110; 1,180; and 1,265 cm^{-1} which can be

Table 1
Adsorption experimental runs

Experimental run	pH	TS-GO (mg/L)	Contact time (min)	AMX and CIP (mg/L)	Temperature (°C)
pH	3–9	50	30	20	25
TS-GO concentration	Optimum	20–200	30	20	25
Contact time	Optimum	Optimum	0–30	20	25
Antibiotics concentration	Optimum	Optimum	30	10–100	25
Solution temperature	Optimum	Optimum	30	100	20–40

assigned to different bonds between carbon and nitrogen in PNVCL/GO including RNH_2, =NOH, R_2NH, and RCO–N [23]. The appearance of bands at 1,627 cm^{-1} belongs to the C=O vibration in the carbonyl group or carboxylic bonds. The broad absorption band in the range of 3,300–3,500 cm^{-1} corresponded to O–H stretching vibrations. The stretching and bending vibrations of aromatic C=C and C–H are also presented at 1,735; 586; and 701 cm^{-1}. Comparing the FTIR spectrum for GO before and after the modification process, shows that the intensity of the O–H band at 3,432 cm^{-1} is changed. This is due to the overlapping of the –OH and $–NH_2$ stretching vibrations by insertion of PNVCL molecules. Also, The peak intensity of C=C, C=O, and the aliphatic C–H at 1,735; 1,627; and 2,923 cm^{-1} is clearly changed, which can suggest the involvement of these functional groups in the formation of TS-GO catalyst.

The morphological investigations of the as-synthesized GO and TS-GO samples were carried out by SEM. Figs. 5a–f show ultra-thin nanosheets of GO with a certain degree of exfoliation and wrinkles. Figs. 6a–f depict that after the compositing process, more exfoliation and wrinkles are created on the surface of GO nanosheets, which indicates PNVCL modification affects the carbon network of GO. The increasing in wrinkles originates from the structural distortion and the created defective sites after the insertion of PNVCL polymer molecules on the surface of GO. This phenomenon offers a maximum benefit from the surface area and more accessible active sites in contact with the surrounding species for adsorption of the pollutants in solutions.

The elemental composition of the as-prepared GO and modified TS-GO samples was investigated through energy dispersive X-ray analysis and the results are illustrated in Figs. 5 and 6. The obtained EDX spectrum for pristine GO as shown in Fig. 5g confirms that it is composed of C and O atoms with an atomic ratio of O/C: 0.083 (O: 7.66%, C: 92.34%), and no other impurities have been found. As shown in Fig. 6g, the elemental composition of TS-GO carries peaks of C, N, O, S, Cl, and K. The presence of N peak confirms the formation of nitrogen-doped GO which are originated from the amine group of PNVCL in the nanocomposite. The EDX spectrum exhibits the good purity level of the TS-GO sample. In addition, the EDX element mappings in Figs. 5h–k and 6h–o demonstrate that the modified ultrathin nanosheets in TS-GO are indeed composited by N and Cl elements of PNVCL.

Figs. 7a and b illustrate the thermogravimetric analysis curves for the as-synthesized TS-GO nanocomposites. It is clear that, the TGA and corresponding DTA curves for the sample had four distinct regions (*A*, *B*, *C*, and *D*). Based on TGA curve (Fig. 7a), the mass loss section (*A*) is mainly related to the dehydration of water in a temperature regime of 80°C–150°C, and section (*B*) mainly corresponds to the melting and degradation of polymeric chains of PNVCL in the region up to 160°C, section (*C*) is mainly due to the loss of amine groups at 350°C–500°C, and section (*D*) the final step is related to the residual carbon of GO [24]. Fig. 7b shows the corresponded DTA curve of TS-GO. As can be seen, it confirms the melting of polymer chain at around 250°C and then, the destruction at up to 250°C. In addition, two distinct decompositions occur at temperature regions around 350°C–800°C and 850°C – up to 1,000°C, indicating the combustion of amine groups and decomposition of carbon residues in GO. The DTA results are in good agreement with TGA.

The pore structure of GO and TS-GO were studied using N_2 adsorption (Fig. 8). The BET surface area and BJH model using desorption branch of the nitrogen isotherm have been employed to obtain the pore size distribution. As can be seen in Fig. 8a, a distinct hysteresis loop at $0 < P/P_0 < 1$ indicated that the materials show type III isotherm due to mesoporosity according to IUPAC classification [25]. The commercial GO material showed a surface area of 11.43 m^2/g and pore size distribution of 2–20 nm with the average of 11.03 nm (Fig. 8b). Meanwhile, the BET surface area of TS-GO (Fig. 8c) was of 53.52 m^2/g belonged to the type III category, indicating that PNVCL polymers lie on the surface and between GO layers and hinder the aggregation of ultra-thin nanosheets which leads to increasing the specific surface area. Fig. 8d shows the pore radius of the TS-GO around 3–20 nm with the average of 17 nm. The results are in good agreement with SEM images, confirming the improvement in surface area and morphology of TS-GO compared with pristine GO, which could lead to an enhancement in the adsorption process.

The stability and dispersion of GO in solution depends strongly on the surface charge, which could be investigated by zeta potential. The surface of graphene oxide contains hydrophilic functional groups including carboxyl group (–COOH) or hydroxyl group (–OH). With dispersion of GO in an aqueous solution, the carboxyl groups can be ionized to carboxylate ($–COO^-$) and also form OH^- anions in an alkaline environment, both cause negatively charged surface of GO [26].

To obtain pH_{zpc} (pH point of Zero Charge), the primary and the final pH of GO suspension have been investigated. NaCl 0.1 M and NaOH 0.1 M solutions were used to adjust primary pH values as: 3, 4, 5, 6, 7, 8, 9, and 10. As shown in Fig. 9, the obtained value of pH_{zpc} for GO was 3.8. Meanwhile, the value of pH_{zpc} for TS-GO sample increased to 7.9, which obviously confirms the effect of the amine functionalized groups on the surface charge of the modified GO. Since TS-GO is in an alkaline environment (due to amine group of PNVCL), its absolute value of pH_{zpc} is larger than that of carboxyl groups [27].

3.2. Adsorption of antibiotics on TS-GO

To investigate the parameters affecting the adsorptive removal processes of AMX and CIP, several independent factors have been optimized, that are sample pH, mass of adsorbent (TS-GO), time, concentration of the contaminants, temperature, and reusability of the modified graphene oxide. The experimental values of analytical response including antibiotic removal efficiency and antibiotic adsorption capacity under various experimental conditions will be discussed.

3.2.1. Effect of pH

pH is an important factor which can determine the catalytic performance of the prepared adsorbent, because the change in pH affects the degree of ionization of TS-GO surface functional groups [13]. The effect of sample pH on the adsorptive removal of AMX and CIP is presented in

Fig. 10a. It can be seen that the removal efficiency of AMX decreased with increasing sample pH up to an optimum value of pH = 3. The related % removal for AMX was 100%, 97%, 92%, 79%, 75%, 67%, and 56% for sample pH of 3, 4, 5, 6, 7, 8, and 9, respectively. Meanwhile, the adsorptive removal of CIP increased with increasing sample pH from 3 to 5 (from 93% to 100% removal efficiency). However, the removal rate decreased after the optimum sample pH and % antibiotic removal for CIP was achieved as 99%, 97%, 85%, and 71% at sample pH values of 6, 7, 8, and 9, respectively. The corresponding adsorbed antibiotic (mg/g) of AMX and CIP over the modified GO adsorbent is illustrated in Fig. 10b. As shown, the highest amount of adsorbed AMX and CIP in the presence of TS-GO was 400 mg/g at sample pH of 3 and 5, respectively. As mentioned above, the amount of adsorbed CIP shows increasing from pH = 3 to 5, and subsequently decreased with the increase of pH values. Such adsorption behavior can be due to the electrostatic interactions between AMX and CIP molecules and ionizable functional groups at the surface of TS-GO such as carboxyl, carbonyl and substitute amine groups from PNVCL. At different pH values, these active groups could involve with protonation–deprotonation reactions, leading to formation of cation, and anion species. On the other hand, at different pH values, the surface charge of the antibiotic molecules could change which highly affect their tendency to the surface of TS-GO adsorbent. The obtained results are in good agreement with previous reports [13,28,29]. For example, Qu and Morais [30] showed at pH > pH_{pzc}, the H^+ ions can leave the surface of adsorbent owing to the partially negative charge of ZnO oxygen atoms. In contrast, at pH < pH_{pzc}, H^+ ions could be transferred to the surface of adsorbent and combine with the OH^- groups, which causes a positive charge of the ZnO surface. The decreased amount of adsorbed antibiotic implies that the surface of the adsorbent has no longer active sites for interaction with antibiotic molecules up to an optimum value of pH.

3.2.2. Influence of initial concentrations and contact time

The influence of the TS-GO concentration on removal efficiency was studied, Figs. 11a and b. The results demonstrated that the % removal and adsorption capacity enhanced with an increase in the concentration of adsorbent from 20 to 50 mg/L for both antibiotics. Based on Fig. 11a, the removal efficiency remained still for upper concentrations between 50 and 200 mg/L. Consequently, the adsorbed amount of antibiotics decreased to 100 mg/g which determines the maximum capacity of TS-GO surface at 50 mg/L.

The effect of initial antibiotic concentrations have been studied in the presence of 50 mg/L TS-GO adsorbent during reaction time of 30 min. The results are depicted in Fig. 11c. The concentrations varied from 10 to 100 mg/L and their removal percentage by TS-GO was tested at pH = 3 and 5 for AMX and CIP, respectively. As seen in the evolution curves, the removal efficiencies of AMX and CIP decreased remarkably with an increase in the initial concentration of the antibiotics, while the adsorbed amount enhanced from 200 mg/g for concentration of 10 mg/L to around 600 mg/g for 100 mg/L of adsorbate (Fig. 11d). This is due to the fact that by increasing the concentration of AMX and CIP, the availability of antibiotic molecules at the adsorbent interface also increases. However, for antibiotic concentrations of up to 60 mg/L the adsorption amount does not change which implies the occupation of all of the active sites on the surface of TS-GO adsorbent. When the surface active sites of TS-GO are covered fully, the adsorption amount reaches a limit which leads to saturated adsorption.

The effect of contact time on AMX and CIP adsorption by TS-GO have been investigated and shown in Figs. 11e and f. The results show that the adsorption of antibiotics is rapid, and more than half the amount of AMX and CIP is removed in the first 5 min, which greatly suggests the as-prepared TS-GO as an efficient adsorbent for removal of contaminants from water. This trend in the adsorption suggests that there is large number of sites available on the TS-GO. [13] As can be seen, the complete removal and maximum amount of adsorbed antibiotics over TS-GO can be achieved during 30 min, and the adsorption reached equilibrium in about 15 min with a maximum adsorbed amount of 380–400 mg/g for 20 mg/L initial AMX and CIP concentration. A similar trend in the contact time and removal efficiency is observed in other studies. For example, Moussavi et al. [13] investigated removal efficiency of acetaminophen using double-oxidized graphene oxide, they also found that the highest removal efficiency of acetaminophen is observed within primary 10 min of the reaction and further increase of the reaction time leads to a negligible increase in removal efficiency.

3.3. Adsorption isotherms

Study of the equilibrium adsorption isotherm is one of the most important steps which can describe how the adsorbate interacts with the surface of adsorbent. The adsorption mechanism could be identified by modeling of isotherms using different equilibrium models [13]. In this work, the two common isotherms including Langmuir and Freundlich models have been employed to explain the experimental adsorption data [31]. In recent years, these two models have been widely reported in literature, regarding to modeling of the experimental results of isotherms in different adsorption systems. The Langmuir isotherm assumes monolayer adsorption which takes place at specific homogeneous sites onto the surface of adsorbent with finite number of active sites with uniform energy and no significant interaction occurs between adsorbent and adsorbate species [32]. The Langmuir isotherm is given as Eq. (3) [13]:

$$q_e = q_{\max} \frac{b \cdot C_e}{1 + b \cdot C_e} \tag{3}$$

where C_e (mg/L) is equilibrium concentration of adsorbate; q_e (mg/g) is the amount of adsorbate adsorbed at equilibrium; $q_{\max}$ (mg/g) is maximum monolayer adsorption capacity; and b is Langmuir constant related to the energy of adsorption (L/mg). The Freundlich isotherm model is used to describe the models of multilayer absorption of species onto the surface of heterogeneous sites. The Freundlich isotherm model is represented by Eq. (4):

$$\ln q_e = \ln K_f + \frac{1}{n} \ln C_e \tag{4}$$

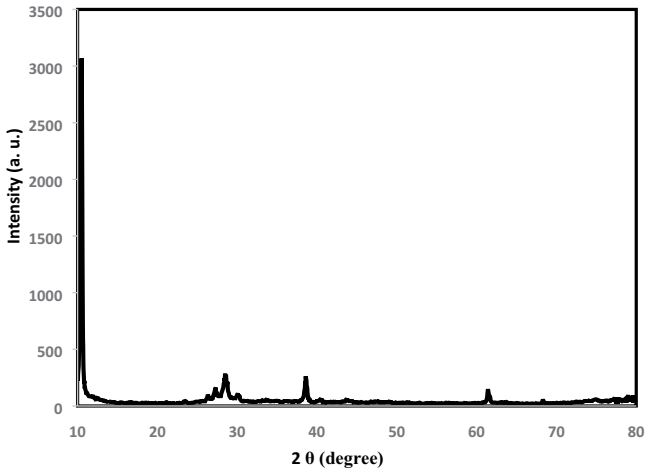

Fig. 1. XRD pattern of GO sample.

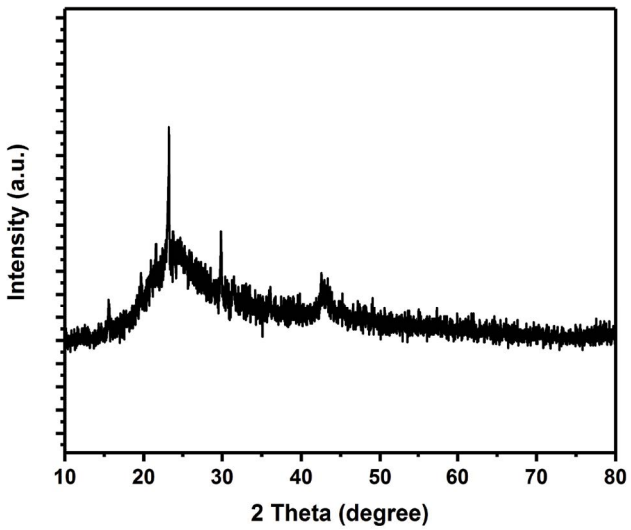

Fig. 2. XRD pattern of the as-prepared TS-GO sample.

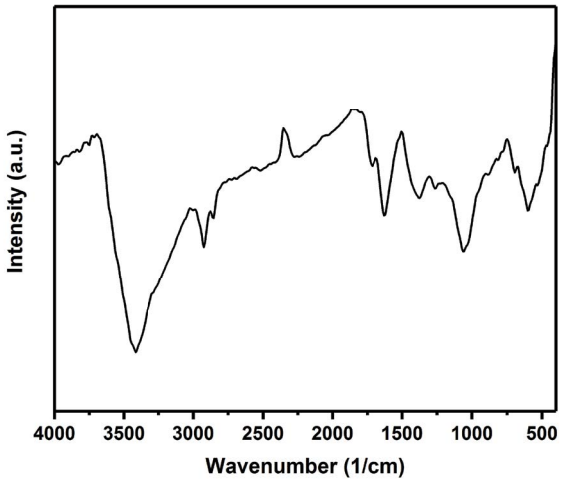

Fig. 3. FTIR spectra of GO.

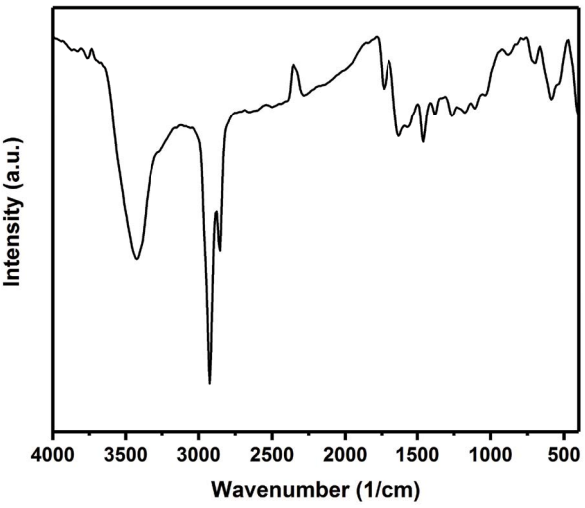

Fig. 4. FTIR spectra of TS-GO sample.

where K_f (L/mg) and n are Freundlich isotherm constants related to saturation capacity of adsorbent and intensity of the adsorption, respectively, q_e is the amount of adsorbate adsorbed at equilibrium (mg/g), and C_e is the residual concentration of antibiotics in the solution at equilibrium (mg/L). Based on previous reports, the value of $1/n$ between 0.1 and 1 depicts a favorable adsorption process [33]. The experimental data were fit with these two models and the constants and correlation coefficients calculated using linear regression, Fig. 12. The results are presented in Table 2. As seen, the maximum monolayer capacity values of AMX and CIP (q_{max}) calculated as 625 and 769.23 mg/g, respectively. These values are larger than AMX and CIP adsorption amounts in various reported absorbents [34–39] which indicate the thermosensitive GO based adsorbent presented in current work is an outstanding candidate for designing new adsorbents for drug pollution removing from water. Table 3 compares the results of present study with similar studies. The values given in the table are based on initial antibiotics concentrations of 20 mg/L. the adsorption capacity in the present study was calculated to be about 400 mg/g in case of an antibiotic initial concentration of 20 mg/L. Increasing the initial concentration of antibiotics to 100 mg/L, showed an increasing in the adsorption capacity, however, considering the five time increase in the initial concentration only led to doubling of the adsorption capacity of the catalyst. This could be due to the high occupation of active sites in the catalyst in the presence of antibiotics.

Regarding to the obtained R^2 and $1/n$ values, the Langmuir isotherm better fits the experimental data compared with Freundlich isotherm model, implying that the adsorption process occurs as a monolayer phenomenon and the adsorption mechanism does not seem to be a multilayer process.

3.3. Adsorption kinetics

To obtain the rate of the reaction, the adsorption kinetics of the AMX and CIP over the smart TS-GO nanosheets have

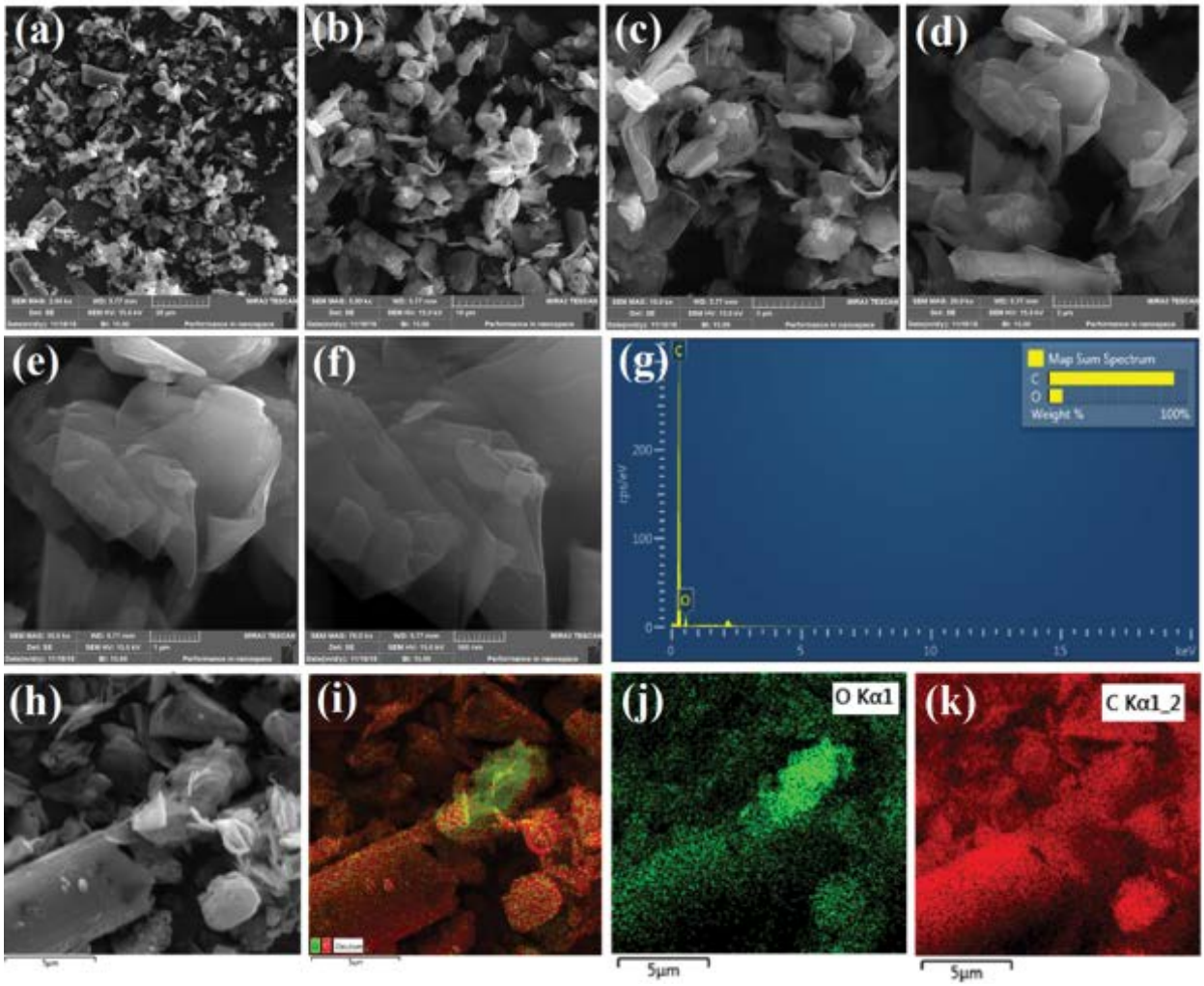

Fig. 5. (a–f) SEM images of GO, (g) EDX element mapping of GO, and (h–k) GO, total, O, and C.

been evaluated by two commonly used pseudo-first-order and pseudo-second-order models which are represented as given below (Eqs. (5) and (6)) [44]:

$$\text{Log}\left(q_e - q_t\right) = \log q_e - K_1 \cdot t \tag{5}$$

$$q_t = q_e\left(\frac{q_e \cdot K_2 \cdot t}{1 + q_e \cdot K_2 \cdot t}\right) \tag{6}$$

where K_1 (L/min) and K_2 (g/mg min) are the pseudo-first-order and pseudo-second-order rate constants, respectively. The results presented in Fig. 13 and Table 4 indicate that the pseudo-second-order kinetic model had the highest correlation coefficient calculated as 0.9894 and 0.9934 for AMX and CIP, respectively. This suggests that for the adsorptive removal of both antibiotics the experimental results fitted better the pseudo-second-order compared with pseudo-first-order kinetic model, which may be due to a rate-limiting step in the adsorption process [44]. Moreover, the calculated q_e from pseudo-second-order model was close to the experimental values of q_e, 476 and 435 mg/g for AMX and CIP, respectively. The rate of AMX and CIP adsorption over TS-GO using pseudo-second-order model was calculated as 0.000172 L/min and 0.000465 g/mg min for two antibiotics.

3.4. Effect of temperature and thermodynamic study

The antibiotic adsorption efficiency was tested as a function of temperature from 20°C to 40°C and the results are shown in Fig. 14. As observed, the increase in temperature had a remarkable impact on the adsorption ability of TS-GO for both antibiotics, and the removal efficiencies of AMX and CIP were highly decreased to less than 20% with the increase in the temperature (at 40°C). This phenomenon can be due to the decreasing of the viscosity of an aqueous solution bearing the pollutant molecules by an increase in the temperature. The decreasing of the viscosity could permit the enhancement of the diffusion rate of the antibiotic molecules (adsorbate) across the external surface and pore boundaries of the TS-GO adsorbent nanosheets [45].

To study the thermodynamic analysis of TS-GO adsorbent for adsorption of AMX and CIP, the thermodynamic parameters including the Gibbs free energy (ΔG°), the

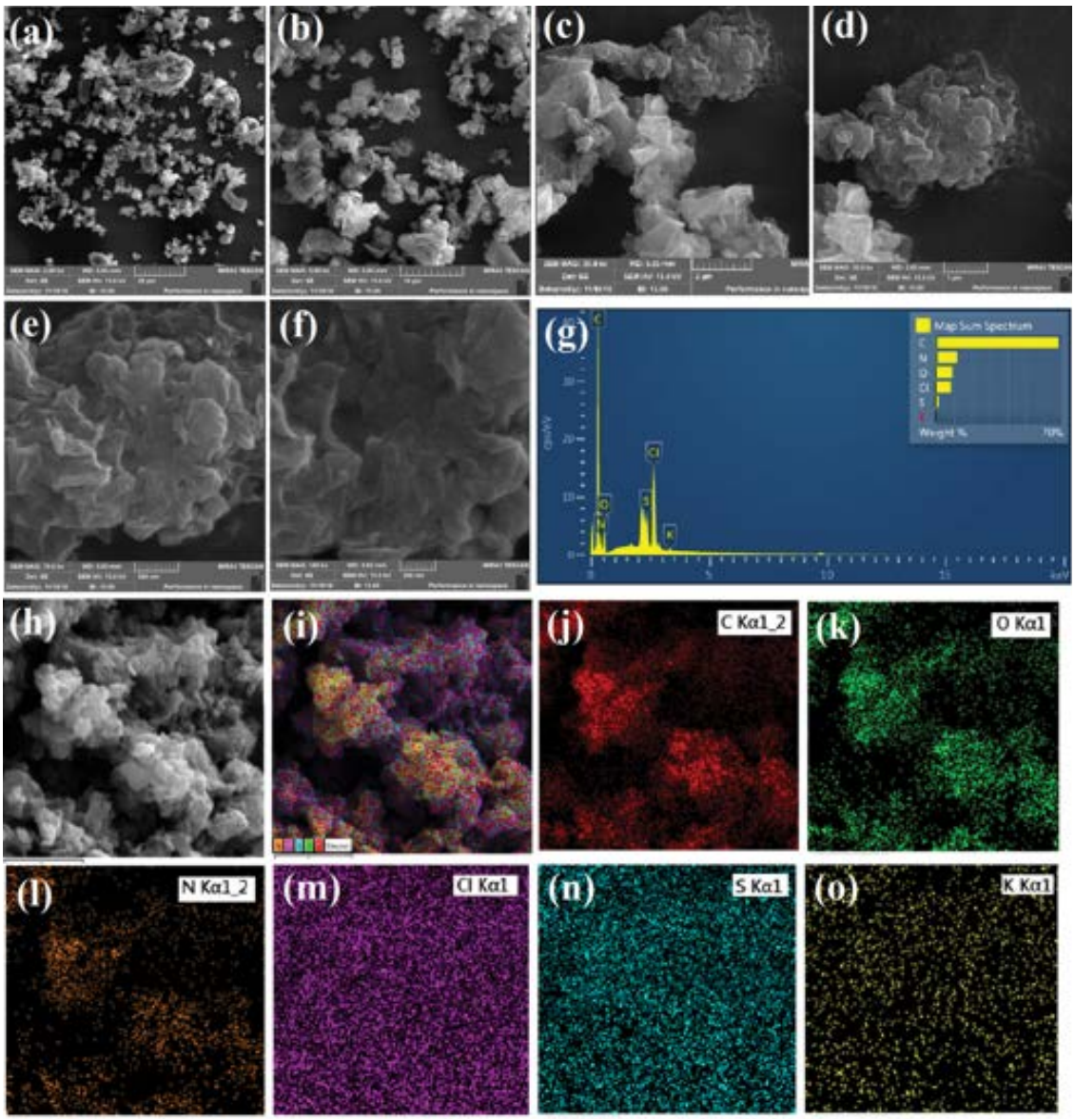

Fig. 6. (a–f) SEM images of the as-prepared TS-GO, (g) EDX element mapping of TS-GO, and (h–o) SEM image of TS-GO, total, C, O, N, Cl, S, and K.

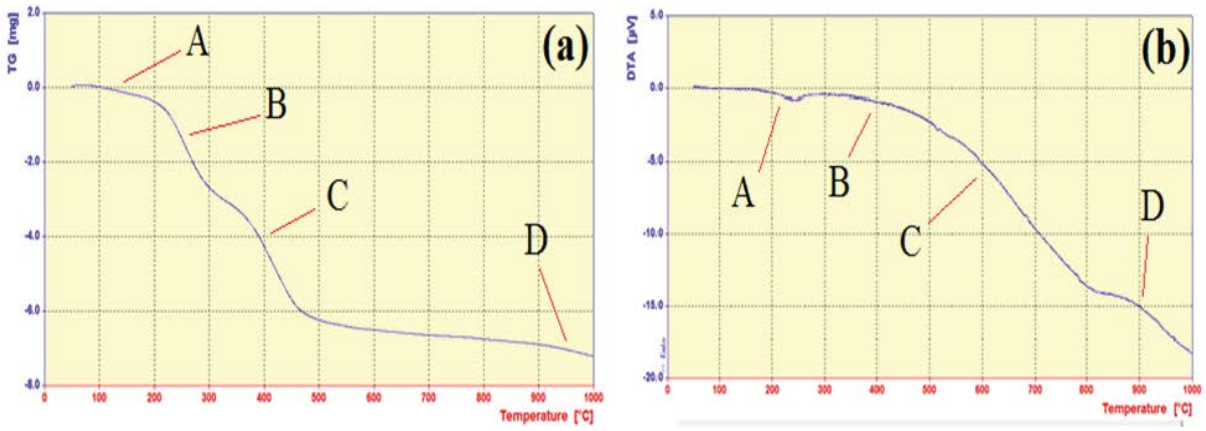

Fig. 7. (a) TGA and (b) DTA of the TS-GO sample.

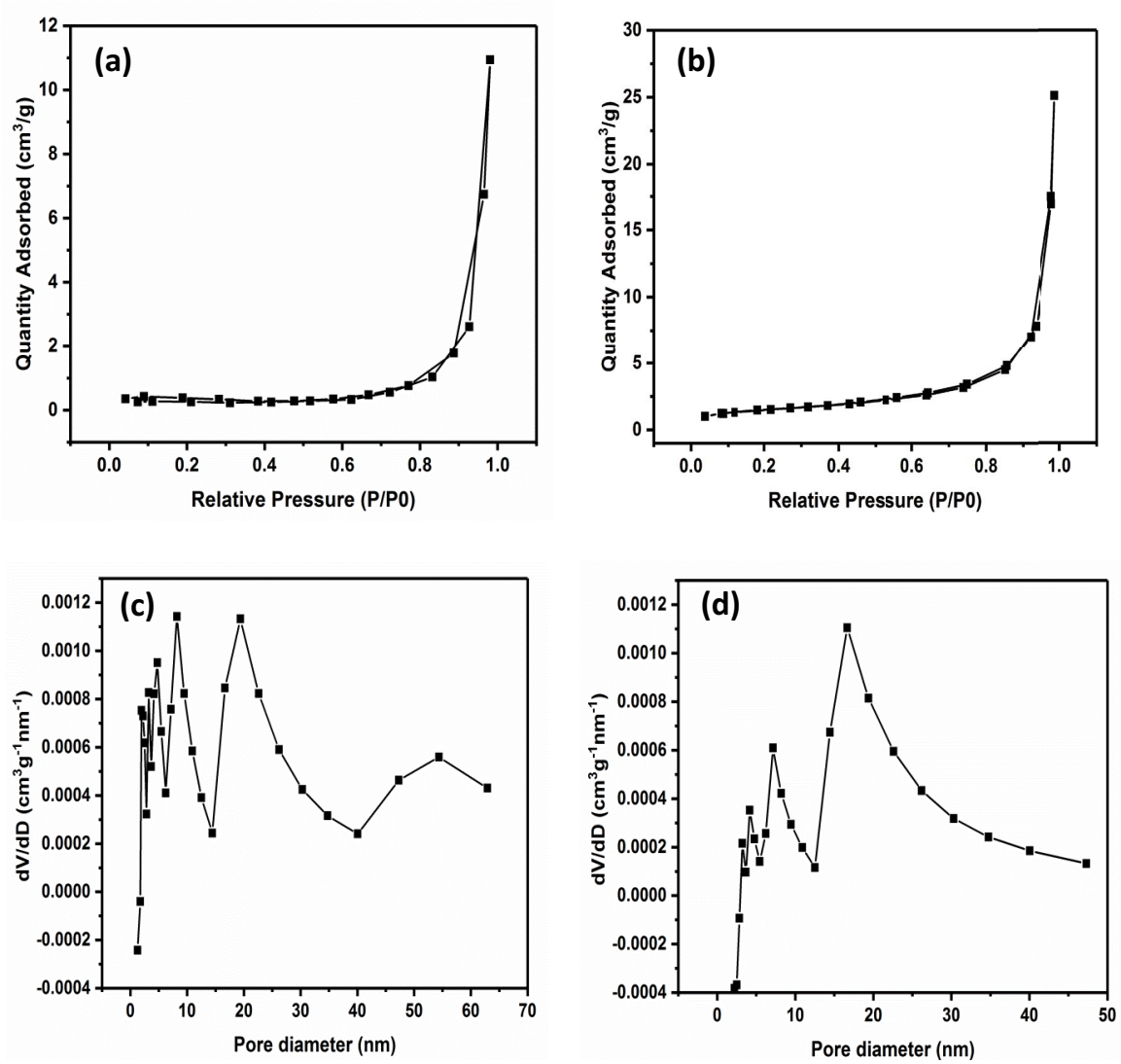

Fig. 8. (a and c) N_2 adsorption and (c and d) pore size distribution of GO and TS-GO.

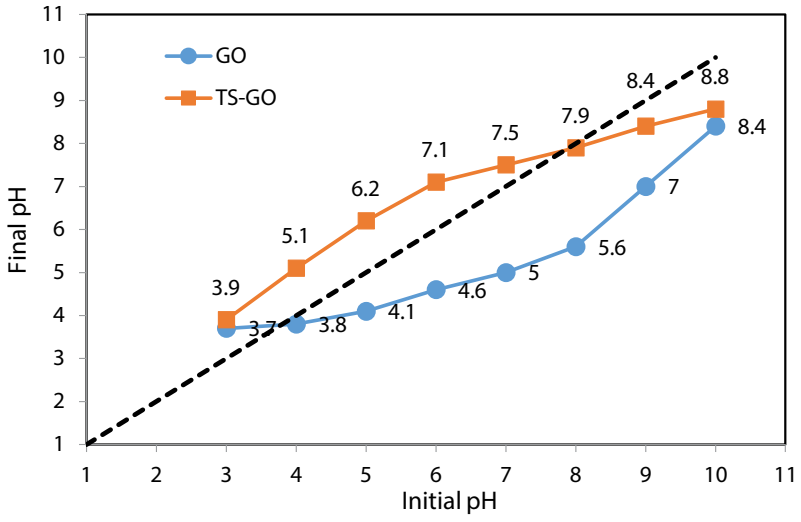

Fig. 9. Value of pH_{zpc} for GO and TS-GO.

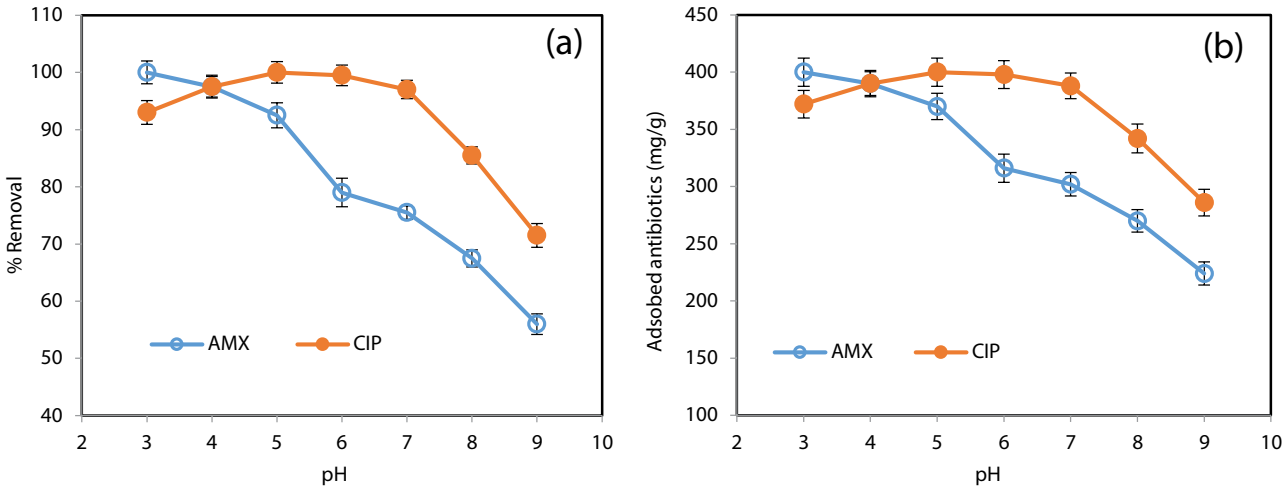

Fig. 10. (a) Effect of pH and (b) the related adsorbed AMX and CIP (AMX and CIP = 20 mg/L, GO = 50 mg/L, and time = 30 min).

Table 2
Calculated isotherm and regression parameters of AMX and CIP onto TS-GO

Model	Parameter	AMX	CIP
Langmuir	q_{max} (mg/g)	625	769.23
	K_L (L/mg)	0.2917	0.078
	R^2	0.9893	0.9777
Freundlich	K_f (mg/g)	1.342	1.152
	$1/n$	2.062	1.777
	R^2	0.8371	0.8665

enthalpy ($\Delta H°$), and the entropy ($\Delta S°$) were calculated using the following equations [46,47]:

$$K_c = \frac{q_e}{C_e} \tag{7}$$

$$\Delta G° = -RT \ln K_c \tag{8}$$

$$\ln K_c = \frac{\Delta S°}{R} - \frac{\Delta H°}{RT} \tag{9}$$

where C_e is the equilibrium concentration (mg/L) of the AMX and CIP solution, q_e is the equilibrium adsorption capacity (mg/g), K_c (L/g) is the equilibrium constant which is equal to the ratio of the adsorbed quantity of antibiotic molecules onto the TS-GO, $\Delta G°$ is the Gibbs free energy change in adsorption (kJ/mol), $\Delta H°$ is the change in enthalpy in adsorption (kJ/mol), $\Delta S°$ is the entropy change in adsorption [kJ/(mol K)], T (K) is the solution temperature, and R is the universal gas constant (8.314 J/K mol). With a linear plot of $\ln K_c$ vs. $1/T$ from the model, the enthalpy entropy change ($\Delta H°$ and $\Delta S°$) can be calculated from the slope and intercept of the van't Hoff plot, Fig. 14, respectively. The calculated thermodynamic parameters are presented in Table 5. As can be seen, q_e and consequently K_c

Table 3
Comparison of AMX and CIP maximum capacity onto different carbonaceous adsorbents

Pharmaceutical	Adsorbents	Dose (g/L)	pH	T (°C)	BET (m^2/g)	Capacity	Reference
Amoxicillin	TS-GO	0.05	3	25	53.52	625* (mg/g)	Present study
	Activated carbon	0.01–1.7	9	45	1,200	233.775 (mg/g)	[40]
	Nanoporous carbons	0.03	4.3	25	1,055	0.56 (mmol/L)	[34]
	Organically modified bentonites	0.125	7	30	13.70	45.03 (mg/g)	[35]
	Activated carbon	1.5	4.98	30	1,092.951	25.055 (mg/g)	[36]
	Quaternized cellulose	0.08	10	65	–	230.89 (mg/g)	[41]
Ciprofloxacin	TS-GO	0.05	5	25	53.52	769* (mg/g)	Present study
	Activated carbon	0.0025	7.5	25	974	300 (mg/g)	[37]
	Activated carbon	0.05	5	25	1,237	231 (mg/g)	[42]
	Magnetic fullerene	2	6	37	336.84	95 (mg/g)	[38]
	ZnO doped biochar	0.01	4	55	915	167.3 (mg/g)	[43]
	Porous graphene hydrogel	0.01	7	70	–	310 (mg/g)	[39]

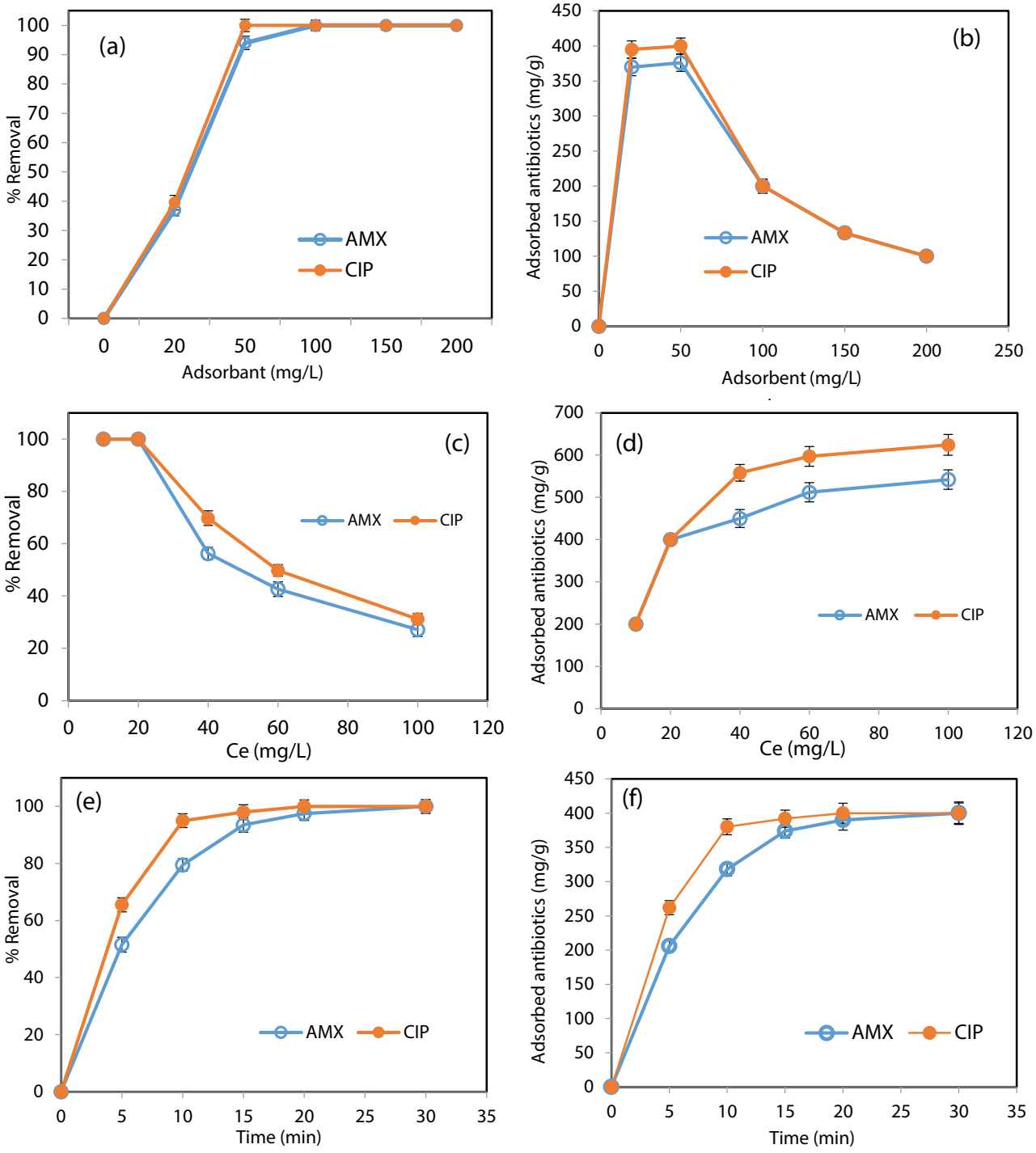

Fig. 11. (a and b) effect of adsorbent dosage; (c and d) effect of initial antibiotics concentration; and (e and f) effect of contact time on the adsorption of AMX and CIP on TS-GO.

decreased with an increase in the temperature from 293 to 313 K, which is not favored for adsorption process. The negative values of $\Delta G°$ for all the temperatures suggests that the adsorption reactions of the AMX and CIP onto TS-GO were spontaneous [48]. In addition, the negative values of $\Delta H°$ and $\Delta S°$ suggest that the nature of the adsorption process was exothermic, and the randomness at the sorbent–solution interface decreases during the reaction of AMX and CIP with the TS-GO nanosheets.

3.5. Reusability

The regeneration of the as-prepared adsorbent is a significant economic factor for the removal of contaminants

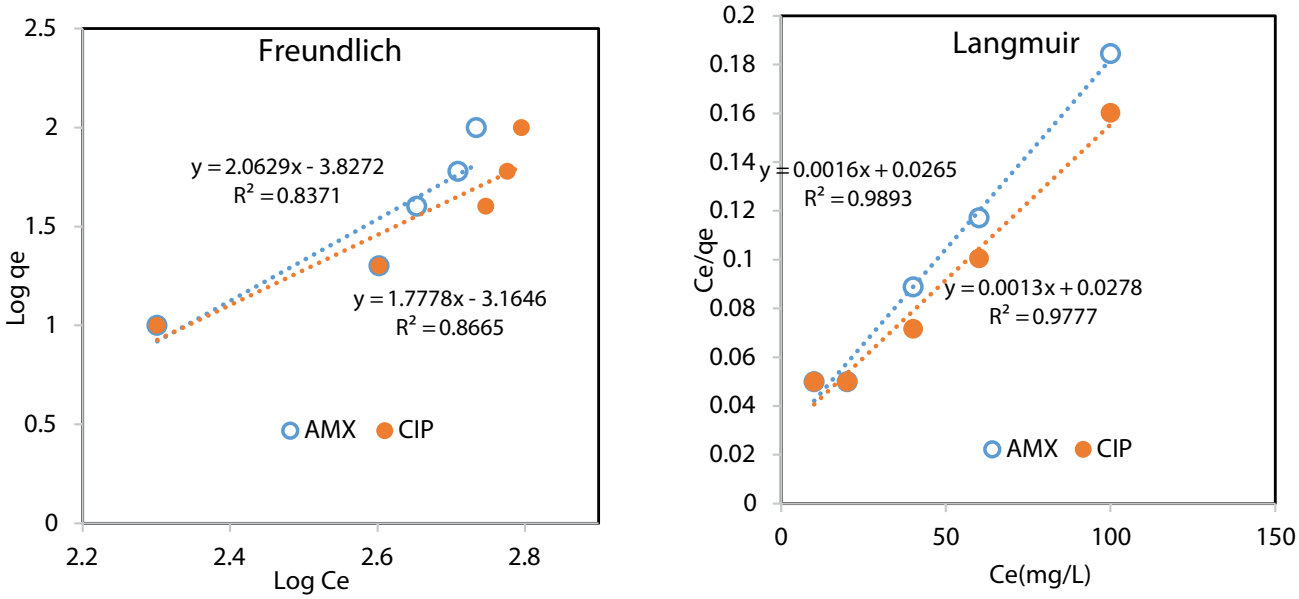

Fig. 12. Adsorption isotherms of AMX and CIP by TS-GO, (TS-GO = 50 mg/L, pH = 3, 5, and t = 30 min).

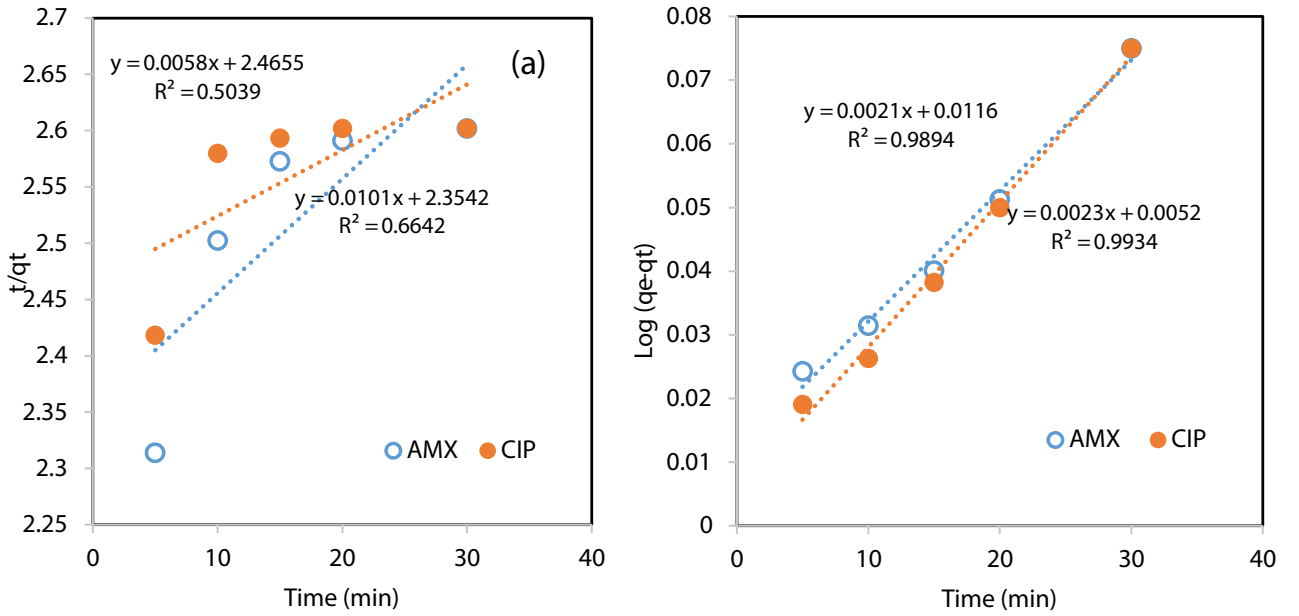

Fig. 13. (a) Pseudo-first-order and (b) pseudo-second-order models at 293 K.

from aqueous solution. In this work, the reusability of the TS-GO adsorbent was studied using the adsorption/desorption experiments to obtain the number of times TS-GO could be used efficiently for the removal of AMX and CIP. Firstly, two different eluent were used to desorb AMX and CIP at temperature of 45°C; methanol and deionized water. At this temperature, the polymeric NVCL which is double bonded to GO by acrylamide, can release the antibiotic molecules from the surface of GO. After drying the powder, the recovered adsorbent was used repeatedly in the next adsorption processes. As shown in Fig. 14b, percentage recoveries obtained ranged from 100% to 90% and 95% for AMX and CIP, respectively, during four cycles of adsorption-desorption experiments. So, it could be concluded that TS-GO is a highly sustainable, reusable, and economical adsorbent, thus making it to be suitable for treatment of wastewater.

3.6. Contribution of TSP in adsorption process

In order to investigate the contribution of TSP on adsorption process, experiments were conducted under optimum condition for GO. At this experiment the antibiotics concentrations wer 20 mg/L and graphene oxide was 50 mg/L. The results are shown in Fig. 15. Fig. 11e also

Table 4
Parameter values of the kinetics models fitting to the experimental data for adsorption of AMX and CIP onto TS-GO. ([adsorbate] = 20 mg/L and adsorbent dosage = 50 mg/L)

Adsorbate	Pseudo-first-order model			Pseudo-second-order model		
	K_1 (L/min)	R^2	q_e (mg/g)	K_2 (g/mg.min)	R^2	q_e (mg/g)
AMX	0.02303	0.6642	0.968	0.000172	0.9894	476.19
CIP	0.01335	0.5039	0.902	0.000465	0.9934	434.78

Table 5
Thermodynamic parameters for the adsorption of AMX and CIP onto TS-GO (initial antibiotic concentration = 20 mg/L, TS-GO dose = 50 mg/L, time = 30 min, pH = 3 and 5 for AMX and CIP, respectively)

			Thermodynamic parameters		
Adsorbate	T (°C)	q_e (mg/g)	ΔG° (kJ/mol)	ΔH° (kJ/mol)	ΔS° (kJ/mol)
	20	400	–97.44008		
	25	374.4	–92.7603		
AMX	30	319.6	–80.51178	–61.7597	–0.177753
	35	207.2	–53.05795		
	40	69.6	–18.11188		
	20	400	–97.44008		
	25	392.4	–97.21993		
CIP	30	369.2	–93.00672	–53.958	–0.150982
	35	278	–71.18779		
	40	79.2	–20.61007		

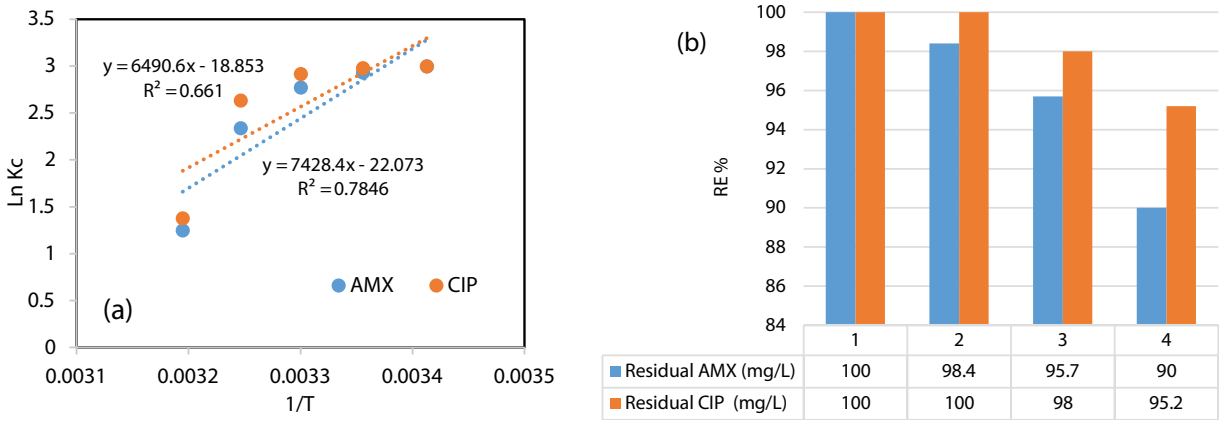

Fig. 14. (a) Thermodynamic investigation of the adsorption of AMX and CIP by TS-GO and (b) reusability of TS-GO during four adsorption runs.

shows the same experimental condition in case of TS-GO. As shown, the antibiotics removal efficiency were higher in case of TS-GO compared to that of GO. In the presence of TS-GO, complete removal of antibiotics is reached within 30 min while only 48.8% and 33.1% of CIP and AMX were removed, respectively. This indicate that TSP was effective in case of increasing the antibiotics removal efficiency. TSP change their physical properties based on the temperature change and induce phase transition [16,20]. Therefore in the optimum temperature, the adsorption of antibiotics using TS-GO is higher than that of GO.

4. Conclusions

In summary, a novel thermosensitive graphene oxide (TS-GO) adsorbent was prepared by mixing graphene oxide nanosheetlets with poly N-vinyl caprolactam (PNVCL), and used for the removal of antibiotic AMX and CIP. This work combines the interaction of surface functionalized amine groups of caprolactam with GO and thermosensitive behavior of PNVCL in desorption of contaminants at 45°C. The modified graphene oxide nanosheetlets were characterized using XRD, FT-IR, SEM, and EDS, which shows the

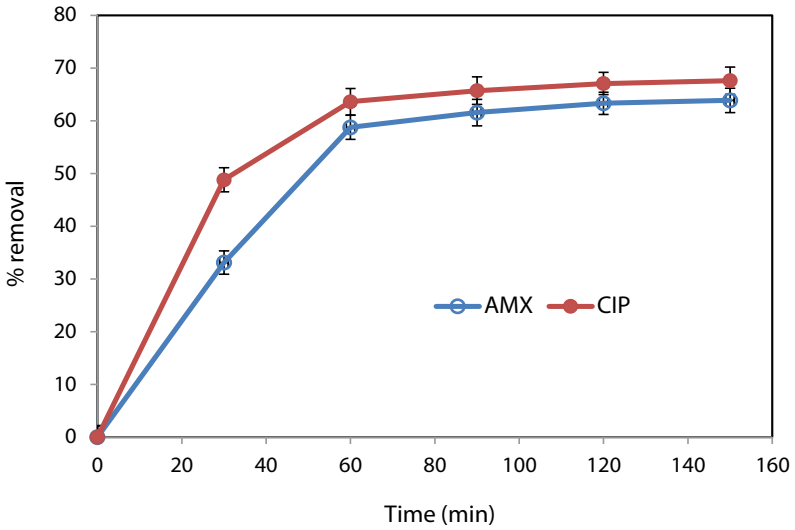

Fig. 15. Adsorption of AMX and CIP on graphene oxide.

effects of the PNVCL on the chemical structure and morphology of GO. The adsorption behavior of TS-GO was investigated by optimizing different factors including sample pH, concentrations, and temperature. The results showed the complete removal of AMX and CIP within 30 min using 50 mg TS-GO at acidic pH values, which suggests the high efficiency of the prepared adsorbent for wastewater treatments. The behavior of AMX and CIP adsorption onto the TS-GO well-fitted the pseudo-second-order kinetic model and Langmuir isotherm. The maximum monolayer capacity values of AMX and CIP (q_{max}) calculated as 625 and 769.23, respectively. Desorption process of antibiotic molecules from the surface of TS-GO mainly belongs to the thermosensitive behavior of smart PNVCL at higher temperatures. The proposed adsorbent with large adsorption capacity is highly promising for applications in the field of wastewater treatment and molecular separations.

Acknowledgments

The authors acknowledge the department of environmental engineering of Azad University for providing necessary research infrastructure and equipment/instruments.

References

[1] D.J. Lapworth, N. Baran, M.E. Stuart, R.S. Ward, Emerging organic contaminants in groundwater: a review of sources, fate and occurrence, Environ. Pollut., 163 (2012) 287–303.
[2] G. Moussavi, M. Rezaei, M. Pourakbar, Comparing VUV and VUV/Fe^{2+} processes for decomposition of cloxacillin antibiotic: degradation rate and pathways, mineralization and by-product analysis, Chem. Eng. J., 332 (2018) 140–149.
[3] B.M. Sharma, J. Bečanová, M. Scheringer, A. Sharma, G.K. Bharat, P.G. Whitehead, J. Klánová, L. Nizzetto, Health and ecological risk assessment of emerging contaminants (pharmaceuticals, personal care products, and artificial sweeteners) in surface and groundwater (drinking water) in the Ganges River Basin, India, Sci. Total Environ., 646 (2019) 1459–1467.
[4] G. Moussavi, M. Pourakbar, S. Shekoohiyan, M. Satari, The photochemical decomposition and detoxification of bisphenol A in the VUV/H_2O_2 process: degradation, mineralization, and cytotoxicity assessment, Chem. Eng. J., 331 (2018) 755–764.
[5] D. Cheng, H.H. Ngo, W. Guo, S.W. Chang, D.D. Nguyen, Y. Liu, Q. Wei, D. Wei, A critical review on antibiotics and hormones in swine wastewater: water pollution problems and control approaches, J. Hazard. Mater., 387 (2020) 1, doi: 10.1016/j.jhazmat.2019.121682.
[6] M. Pourakbar, G. Moussavi, S. Shekoohiyan, Homogenous VUV advanced oxidation process for enhanced degradation and mineralization of antibiotics in contaminated water, Ecotoxicol. Environ. Saf., 125 (2016) 72–77.
[7] S. Esplugas, D.M. Bila, L.G.T. Krause, M. Dezotti, Ozonation and advanced oxidation technologies to remove endocrine disrupting chemicals (EDCs) and pharmaceuticals and personal care products (PPCPs) in water effluents, J. Hazard. Mater., 149 (2007) 631–642.
[8] O.A. Alsager, M.N. Alnajrani, H.A. Abuelizz, I.A. Aldaghmani, Removal of antibiotics from water and waste milk by ozonation: kinetics, byproducts, and antimicrobial activity, Ecotoxicol. Environ. Saf., 158 (2018) 114–122.
[9] T. Wang, X. Pan, W. Ben, J. Wang, P. Hou, Z. Qiang, Adsorptive removal of antibiotics from water using magnetic ion exchange resin, J. Environ. Sci., 52 (2017) 111–117.
[10] K. Yaghmaeian, G. Moussavi, A. Alahabadi, Removal of amoxicillin from contaminated water using NH_4Cl-activated carbon: continuous flow fixed-bed adsorption and catalytic ozonation regeneration, Chem. Eng. J., 236 (2014) 538–544.
[11] M.-f. Li, Y.-g. Liu, G.-m. Zeng, N. Liu, S.-b. Liu, Graphene and graphene-based nanocomposites used for antibiotics removal in water treatment: a review, Chemosphere, 226 (2019) 360–380.
[12] H. Chen, B. Gao, H. Li, Removal of sulfamethoxazole and ciprofloxacin from aqueous solutions by graphene oxide, J. Hazard. Mater., 282 (2015) 201–207.
[13] G. Moussavi, Z. Hossaini, M. Pourakbar, High-rate adsorption of acetaminophen from the contaminated water onto double-oxidized graphene oxide, Chem. Eng. J., 287 (2016) 665–673.
[14] J. Miao, F. Wang, Y. Chen, Y. Zhu, Y. Zhou, S. Zhang, The adsorption performance of tetracyclines on magnetic graphene oxide: a novel antibiotics absorbent, Appl. Surf. Sci., 475 (2019) 549–558.
[15] R. Rostamian, H. Behnejad, A comprehensive adsorption study and modeling of antibiotics as a pharmaceutical waste by graphene oxide nanosheets, Ecotoxicol. Environ. Saf., 147 (2018) 117–123.
[16] P. Zarrintaj, M. Jouyandeh, M.R. Ganjali, B.S. Hadavand, M. Mozafari, S.S. Sheiko, M. Vatankhah-Varnoosfaderani,

T.J. Gutiérrez, M.R. Saeb, Thermo-sensitive polymers in medicine: a review, Eur. Polym. J., 117 (2019) 402–423.
[17] W.S. Hummers, R.E. Offeman, Preparation of graphitic oxide, J. Am. Chem. Soc., 80 (1957) 1339, doi: 10.1021/ja01539a017.
[18] S.D. Perera, R.G. Mariano, K. Vu, N. Nour, O. Seitz, Y. Chabal, K.J. Balkus, Hydrothermal synthesis of graphene-TiO_2 nanotube composites with enhanced photocatalytic activity, ACS Catal., 2 (2012) 949–956.
[19] Y. Chen, Y. Niu, T. Tian, J. Zhang, Y. Wang, Y. Li, L.-C. Qin, Microbial reduction of graphene oxide by *Azotobacter chroococcum*, Chem. Phys. Lett., 677 (2017) 143–147.
[20] A. Morfin-Gutiérrez, H.I. Meléndez-Ortiz, B.A. Puente-Urbina, L.A. García-Cerda, Synthesis of poly(N-vinylcaprolactam)-grafted magnetite nanocomposites for magnetic hyperthermia, J. Nanomater., 2018 (2018) 3–4.
[21] Z. Bo, X. Shuai, S. Mao, H. Yang, J. Qian, J. Chen, J. Yan, K. Cen, Green preparation of reduced graphene oxide for sensing and energy storage applications, Sci. Rep., 4 (2014) 3, doi: 10.1038/srep04684.
[22] M.Z. Ansari, W.A. Siddiqui, Deoxygenation of graphene oxide using biocompatible reducing agent *Ficus carica* (dried ripe fig), J. Nanostruct. Chem., 8 (2018) 431–440.
[23] S. Kozanoğlu, T. Özdemir, A. Usanmaz, Polymerization of N-vinylcaprolactam and characterization of poly(N-vinylcaprolactam), J. Macromol. Sci. Part A Pure Appl. Chem., 48 (2011) 467–477.
[24] M.D. Pravin, S.F. Chris, A. Gnanamani, Preparation, characterization and reusability efficacy of amine-functionalized graphene oxide-polyphenol oxidase complex for removal of phenol from aqueous phase, RSC Adv., 8 (2018) 38416–38424.
[25] M. Naderi, Chapter 14 - Surface Area: Brunauer–Emmett–Teller (BET), S. Tarleton, Ed., Progress in Filtration and Separation, Academic Press, Oxford, 2015, pp. 585–608.
[26] A.Y.S. Eng, C.K. Chua, M. Pumera, Refinements to the structure of graphite oxide: absolute quantification of functional groups via selective labelling, Nanoscale, 7 (2015) 20256–20266.
[27] A.I. Abd-Elhamid, E.A. Kamoun, A.A. El-Shanshory, H.M.A. Soliman, H.F. Aly, Evaluation of graphene oxide-activated carbon as effective composite adsorbent toward the removal of cationic dyes: composite preparation, characterization and adsorption parameters, J. Mol. Liq., 279 (2019) 530–539.
[28] L.-C. Hsu, Y.-T. Liu, C.-H. Syu, M.-H. Huang, Y.-M. Tzou, H.Y. Teah, Adsorption of tetracycline on Fe (hydr)oxides: effects of pH and metal cation (Cu^{2+}, Zn^{2+} and Al^{3+}) addition in various molar ratios, R. Soc. Open Sci., 5 (2018) 4–7, doi: 10.1098/rsos.171941.
[29] Q. Fanyao, P.C. Morais, The pH dependence of the surface charge density in oxide-based semiconductor nanoparticles immersed in aqueous solution, IEEE Trans. Magn., 37 (2001) 2654–2656.
[30] F. Qu, P.C. Morais, Energy levels in metal oxide semiconductor quantum dots in water-based colloids, J. Chem. Phys., 111 (1999) 8588, doi: 10.1063/1.480200.
[31] D. Balarak, J. Jaafari, G. Hassani, Y. Mahdavi, I. Tyagi, S. Agarwal, V.K. Gupta, The use of low-cost adsorbent (Canola residues) for the adsorption of methylene blue from aqueous solution: isotherm, kinetic and thermodynamic studies, Colloid Interface Sci. Commun., 7 (2015) 16–19.
[32] A.A. Abdullah, N. Mu, A. Tansir, A. Mohammad, A. Ahmed, U. Hasan, K.S. Sudheesh, Removal of highly toxic Cd(II) metal ions from aqueous medium using magnetic nanocomposite: adsorption kinetics, isotherm and thermodynamics, Desal. Water Treat., 181 (2020) 355–361.
[33] Ö. Kerkez, Ş.S. Bayazit, Magnetite decorated multi-walled carbon nanotubes for removal of toxic dyes from aqueous solutions, J. Nanopart. Res., 16 (2014) 2431, doi: 10.1007/s11051-014-2431-1.
[34] H. Mansouri, R.J. Carmona, A. Gomis-Berenguer, S. Souissi-Najar, A. Ouederni, C.O. Ania, Competitive adsorption of ibuprofen and amoxicillin mixtures from aqueous solution on activated carbons, J. Colloid Interface Sci., 449 (2015) 252–260.
[35] E.K. Putra, R. Pranowo, J. Sunarso, N. Indraswati, S. Ismadji, Performance of activated carbon and bentonite for adsorption of amoxicillin from wastewater: mechanisms, isotherms and kinetics, Water Res., 43 (2009) 2419–2430.
[36] S.x. Zha, Y. Zhou, X. Jin, Z. Chen, The removal of amoxicillin from wastewater using organobentonite, J. Environ. Manage., 129 (2013) 569–576.
[37] S.A.C. Carabineiro, T. Thavorn-Amornsri, M.F.R. Pereira, J.L. Figueiredo, Adsorption of ciprofloxacin on surface-modified carbon materials, Water Res., 45 (2011) 4583–4591.
[38] N.A. Elessawy, M. Elnouby, M.H. Gouda, H.A. Hamad, N.A. Taha, M. Gouda, M.S. Mohy Eldin, Ciprofloxacin removal using magnetic fullerene nanocomposite obtained from sustainable PET bottle wastes: adsorption process optimization, kinetics, isotherm, regeneration and recycling studies, Chemosphere, 239 (2020) 6, doi: 10.1016/j.chemosphere.2019.124728.
[39] F. Yu, Y. Sun, M. Yang, J. Ma, Adsorption mechanism and effect of moisture contents on ciprofloxacin removal by three-dimensional porous graphene hydrogel, J. Hazard. Mater., 374 (2019) 195–202.
[40] S. Budyanto, S. Soedjono, W. Irawaty, N. Indraswati, Studies of adsorption equilibria and kinetics of amoxicillin from simulated wastewater using activated carbon and natural bentonite, J. Environ. Prot. Sci., 2 (2008) 72–80.
[41] D. Hu, L. Wang, Adsorption of amoxicillin onto quaternized cellulose from flax noil: kinetic, equilibrium and thermodynamic study, J. Taiwan Inst. Chem. Eng., 64 (2016) 227–234.
[42] S.A.C. Carabineiro, T. Thavorn-amornsri, M.F.R. Pereira, P. Serp, J.L. Figueiredo, Comparison between activated carbon, carbon xerogel and carbon nanotubes for the adsorption of the antibiotic ciprofloxacin, Catal. Today, 186 (2012) 29–34.
[43] Y. Hu, Y. Zhu, Y. Zhang, T. Lin, G. Zeng, S. Zhang, Y. Wang, W. He, M. Zhang, H. Long, An efficient adsorbent: simultaneous activated and magnetic ZnO doped biochar derived from camphor leaves for ciprofloxacin adsorption, Bioresour. Technol., 288 (2019) 2–3, doi: 10.1016/j.biortech.2019.121511.
[44] J. Kunjan, K. Shyam, J. Virendra, Adsorption study of F^- ions onto ultrasonified electrochemically generated ultrafine particles, Desal. Water Treat., 173 (2020) 243–254.
[45] A.A. Mohammed, A.A. Najim, T.J. Al-Musawi, A.I. Alwared, Adsorptive performance of a mixture of three nonliving algae classes for nickel remediation in synthesized wastewater, J. Environ. Health Sci. Eng., 17 (2019) 529–538.
[46] H. Phuong-Thao, N. Ngoc-Tuan, V.H. Nguyen, N. Phuong-Tung, N.T. Duy, D. Van-Phuc, Modeling and optimization of biosorption of lead(II) ions from aqueous solution onto pine leaves (*Pinus kesiya*) using response surface methodology, Desal. Water Treat., 173 (2020) 383–393.
[47] T.M. Albayati, A.A. Sabri, D.B. Abed, Functionalized SBA-15 by amine group for removal of Ni(II) heavy metal ion in the batch adsorption system, Desal. Water Treat., 174 (2020) 301–310.
[48] S. Agarwal, I. Tyagi, V.K. Gupta, M.H. Dehghani, J. Jaafari, D. Balarak, M. Asif, Rapid removal of noxious nickel(II) using novel γ-alumina nanoparticles and multiwalled carbon nanotubes: kinetic and isotherm studies, J. Mol. Liq., 224 (2016) 618–623.